Proceedings of the 2006 WSEAS/IASME International Conference on Fluid Mechanics, Miami, Florida, USA, January 18-20, 2006 (pp25-30)

Numerical Simulation of Turbulent Flow inside the Electrostatic Precipitator of a Power Plant

S.M.E. Haque[1*], M.G. Rasul[2], A. Deev[1], M.M.K. Khan[2] and J. Zhou[3]

[1]Process Engineering & Light Metals (PELM) Centre,
Faculty of Engineering and Physical Systems
Central Queensland University
Gladstone, Queensland 4680
AUSTRALIA

[2]School of Advanced Technologies and Processes
Faculty of Engineering and Physical Systems
Central Queensland University
Rockhampton, Queensland 4702
AUSTRALIA

[3]Stanwell Corporation Limited, Capricorn Highway via Gracemere
Queensland 4702
AUSTRALIA

Abstract: - The performance of Electrostatic Precipitator (ESP) is significantly affected by complex flow distribution. In this study the flue gas flow through the ESP at a local power station is modelled numerically using computational fluid dynamics (CFD) code Fluent to give insight to the flow behavior inside the ESP. The flow simulation was performed using the Reynolds Stress Model (RSM). The prediction of the flow behaviour is compared and discussed with on-site data supplied by the power plant.

Key-Words: - Electrostatic precipitator; Numerical simulation; Fluent; Reynolds Stress Model; Flow distribution

1 Introduction

Particulate matter emission is one of the major air pollution problems of coal fired power plants. Though fine particles constitute a smaller fraction by weight of the total suspended particle matter in typical particle emissions, they are considered potentially hazardous to health because of their high probability of deposition in deeper parts of the respiratory tract. Electrostatic precipitators (ESP) are the most common, effective and reliable particulate control devices which can handle large gas volumes with a wide range of inlet temperatures, pressures, dust volumes and acid gas conditions. Though the electrostatic precipitators are generally running at the collection efficiency as high as 99.95%, the anticipated regulations on particulate matters of 2.5 microns (PM2.5) have led the local power station to explore improvement options to further control the emissions of the fine particulate at a minimum cost even its current particulates emissions are well under the limits of its current environmental license.

The flow distribution within the ESP has been reported to have varying effects on its fly ash particles capture performance depending on the size and arrangement of a ESP. It has been extremely difficult to fully evaluate the flow impact on individual ESP performance until CFD becomes available. CFD plays an ever increasing important role in predicting the flow field characteristics and particle trajectories inside the ESP and optimizing flow distributions within ESP by simulating proposed modification, which ensure that the required flow profiles are achieved – thus substantially reducing the

outage time. However there is a limited research found in the literature for the prediction of turbulent flow behavior inside the ESP. Most of them used standard k-ε turbulence model. Schwab and Johnson [1] developed a numerical flow model of an ESP but did not create any physical geometry for the collection plates. They assumed flow resistance to represent the geometry. Varonos *et al.* [2] developed a model which takes into account the electric-field properties and the particle dynamics along with the basic fluid flow. They introduced flow resistance instead of creating any physical collecting plates. Bottner and Sommerfeld [3] assumed in their model that particle charge was not varying with particle size or particle residence time. Gan and Riffat [4] predict the pressures loss coefficient of orifice and perforated plates. But the hole sizes in the plate are not specifically modeled rather they simplified the perforated plate with a plate of square holes of the same free area ratio. A laboratory scale ESP developed by Nikas *et al.* [5] gave emphasis on the impact of the ionic wind on the gas flow. Dumont and Mudry [6] made a comparative study on flow simulation results from different precipitator CFD models with actual field measurements of velocity patterns.

The aim of this paper is to describe a detail numerical method and an approach adopted to predict the flow pattern inside a full scale ESP. The results of the simulation are discussed and compared with the on-site measured data.

2 Geometry of ESP

The power station in this study has 4 power generating units of 350 MW capacity each. Each unit has 2 single-stage, plate-type, rigid-frame, cold-side and dry ESPs which are called as pass A and pass B. Each pass has two streamlines covering 4 zones as shown in Fig.1. The effective length, width and height of each casing are 30.36m, 22m and 13.1m respectively. The width and height of the Collecting Electrode (CE) wall are 5.76m and 12.5m respectively. Each CE wall is made of 12 CE plates. Each pass has 54 passages having 400mm CE wall spacing. Discharge electrodes (DE) are welded into pipe frames with 2 frames per passage. The width of DE frame is 5.76m and the heights are 5m and 7.5m. Dust removal method for both collection electrodes and discharge electrodes is rapping. Three perforated plates are located within the inlet evase to establish good fluid flow distribution inside the ESP. Due the symmetry in geometry the numerical model is constructed to represent only one-half of a pass. It is to be noted that all the collection plates are taken into account in this three dimensional model and have not been replaced by any equivalent resistance coefficient as other researchers have done in their studies. [1][2] Fig.1 shows the geometrical representation of the ESP.

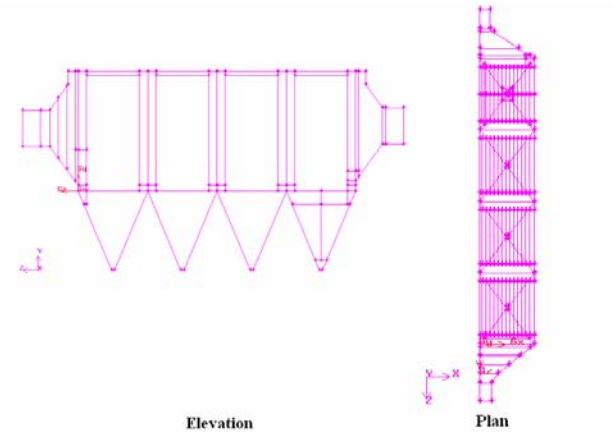

Fig.1 ESP configuration

3 Numerical Approach

Numerical computation of fluid transport includes conservation of mass, momentum and energy, chemical species concentration and turbulence models. Gambit is used as a preprocessor to create the geometry, discretize the fluid domain into small cells to form a volume mesh or grid and set up the appropriate boundary conditions. The flow properties are then specified and the problems are solved and analyzed by FLUENT solver.

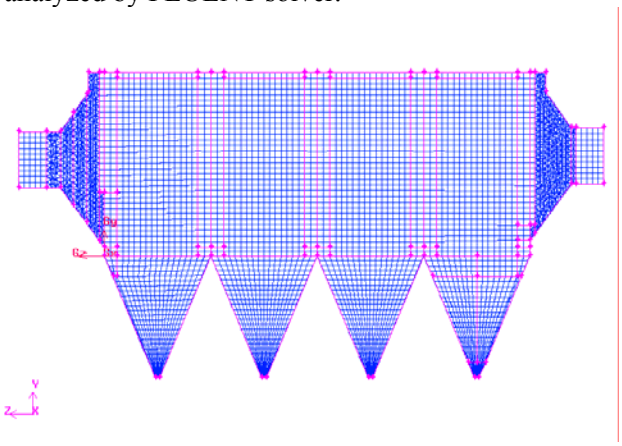

Fig.2 Numerical grid for ESP

The basis of modeling of an incompressible Newtonian fluid flow module is the use of the conservation of mass equations [7]

$$\frac{\partial \rho}{\partial t} + \vec{\nabla} \cdot (\rho \vec{V}) = 0 \quad (1)$$

and the Navier-Stokes equation in x, y and z direction [7]

$$\frac{\partial (\rho u)}{\partial t} + \vec{V} \cdot \vec{\nabla}(\rho u) = -\frac{\partial p}{\partial x} + \vec{\nabla} \cdot (\mu \vec{\nabla} u) + \rho g_x \quad (2)$$

$$\frac{\partial (\rho v)}{\partial t} + \vec{V} \cdot \vec{\nabla}(\rho v) = -\frac{\partial p}{\partial y} + \vec{\nabla} \cdot (\mu \vec{\nabla} v) + \rho g_y \quad (3)$$

$$\frac{\partial (\rho w)}{\partial t} + \vec{V} \cdot \vec{\nabla}(\rho w) = -\frac{\partial p}{\partial z} + \vec{\nabla} \cdot (\mu \vec{\nabla} w) + \rho g_z \quad (4)$$

For the turbulent flow in ESPs, the key to the success of CFD lies with the accurate description of the turbulent behavior of the flow [2]. To model the turbulent flow in an ESP, there are a number of turbulence models available in Fluent. The Reynolds stress model (RSM) is the most elaborate turbulence model that Fluent provides. The RSM involves the Reynolds-averaged Navier-Stokes equations by solving transport equations for the Reynolds stresses, together with an equation for the dissipation rate. The exact transport equations for the transport of the Reynolds stresses, $\rho \overline{u_i' u_j'}$, may be written as follows [8],

$$\frac{\partial}{\partial t}(\rho \overline{u_i' u_j'}) + \frac{\partial}{\partial x_k}(\rho u_k \overline{u_i' u_j'}) =$$
$$-\frac{\partial}{\partial x_k}[\rho \overline{u_i' u_j' u_k'} + \overline{p(\delta_{kj} u_i' + \delta_{ik} u_j')}]$$
$$+\frac{\partial}{\partial x_k}[\mu \frac{\partial}{\partial x_k}(\overline{u_i' u_j'})] - \rho(\overline{u_i' u_k'} \frac{\partial u_j}{\partial x_k} + \overline{u_j' u_k'} \frac{\partial u_i}{\partial x_k})$$
$$-\rho\beta(g_i \overline{u_j' \theta} + g_j \overline{u_i' \theta}) + \overline{p(\frac{\partial u_i'}{\partial x_j} + \frac{\partial u_j'}{\partial x_i})}$$
$$-2\mu \frac{\partial u_i}{\partial x_k} \frac{\partial u_j}{\partial x_k} - 2\rho\Omega_k(\overline{u_j' u_m'} \varepsilon_{ikm} + \overline{u_j' u_m'} \varepsilon_{jkm}) + S \quad (5)$$

where the first and second term of the left hand side represent the rate of increase of $\rho \overline{u_i' u_j'}$ and net rate of flow of $\rho \overline{u_i' u_j'}$ in the fluid element (convection) respectively. The right hand side of the equation contains the terms for turbulent and molecular diffusion, stress and buoyancy production, pressure strain, dissipation, production by system rotation and a user defined source.

The source term is added to the equation for the pressure drop across the perforated plate. In the CFD simulation, the perforated plate is modeled as thin porous media of finite thickness with directional permeability over which the pressure change is defined as a combination of Darcy's Law and an inertial loss term [8].

$$\Delta p = -(\frac{\mu}{\alpha} v + C_2 \frac{1}{2} \rho v^2) \Delta m \quad (6)$$

Where μ is the laminar fluid viscosity, α is the permeability of the plate, C_2 is the pressure loss coefficient per unit thickness of the plate, v is the velocity normal to the porous face and Δm is the thickness of the plate. Appropriate values for α and C_2 are calculated by conducting a separate CFD study on the perforated plate to extrapolate pressure drop against velocity through the perforated plate.

The finite volume methods have been used to discretize the partial differential equations of the model using the simple method for pressure–velocity coupling and the second order upwind scheme to interpolate the variables on the surface of the control volume. The segregated solution algorithm was selected. The Reynolds stress turbulence model was used in this model due to the anisotropic nature of the turbulence in ESPs. Standard fluent wall functions were applied. The input parameters were inlet velocity, turbulence intensity, and hydraulic diameter. Kinetic energy or turbulence intensity was chosen as Reynolds stress specification method. The CFD simulation was performed with a Pentium IV 1.8 GHz 32bit CPU workstation with 512MB RAM-memory and 21GB hard disc memory.

4 Results and Discussions

The operating conditions used for the numerical model are based upon available test data taken at inlet and outlet duct and inside the collection

chamber with the unit offline and the ID fans operating. A windmill vane type anemometer was used to measure the velocity at different planes inside the casing. A volumetric flow rate of 370m^3/s at an average temperature of 24^{0}C was measured with the flow rates from each unit being fairly symmetrical [9]. Measurement of the velocity inside the ESP was carried out for the velocity of 9.36m/s at plane1 as shown in Fig.3 which is set as inlet velocity of the CFD model.

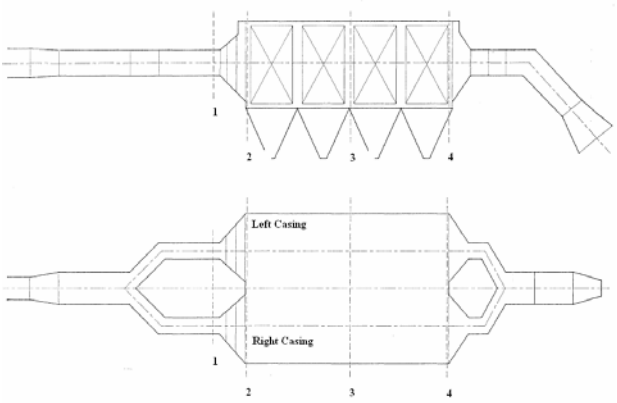

Fig.3 Measurement planes for velocity distribution

Three perforated plates of 8mm, 2mm and 2mm are located inside the inlet evase. A separate CFD study was done placing a small piece of the original perforated plate which is shown in Fig.4 inside a round duct to predict the pressure drop against the perforated plate. Fig.5 represents the predicted pressure drop for the perforated plate for the velocity ranging from 0 to 11m/s. A typical pressure drop curve using the velocity of 10m/s is shown in Fig.6. The curve drawn through the data points in Fig.5 gives an equation which is then compared with equation (6) to obtain the value for α and C_2 for different thickness.

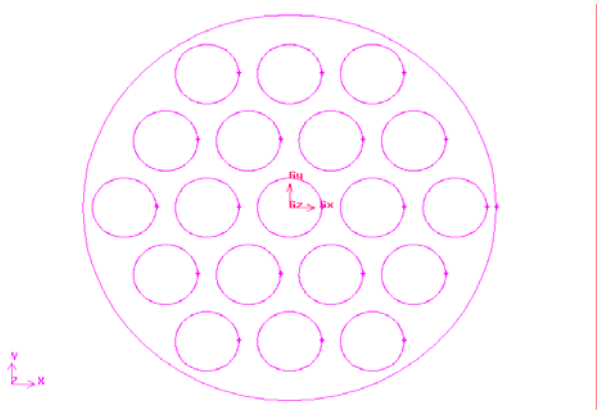

Fig.4 Perforated plate configuration

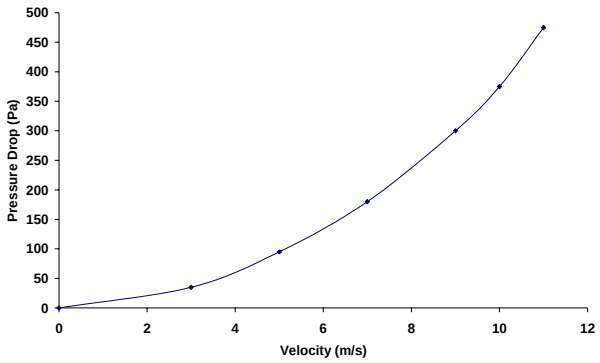

Fig.5 Effect of velocity on the pressure drop for the perforated plate

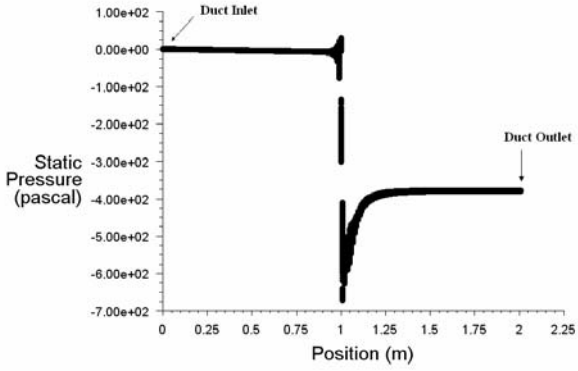

Fig.6 Predicted static pressure drop for the perforated plate (velocity 10m/s)

The numerical model results that have been found are presented in Fig.7, Fig.8 and Fig.9. The predicted velocity at height y=5.91m of plane 2, 3 and 4, shown in Fig.3 is compared with the measured velocity. Fig.10 presents the comparison at plane2 which gives a reasonably good prediction with a maximum deviation of about 20% on the measured values. However the predictions at plane 3, shown in Fig.11 and that at plane 4, seen in Fig.12 do not follow the same trendlines with the measured data. This mismatch may be attributed to a lack of details in the numerical grid to represent the exact geometry and to the influence of flow angularity [3] on the accuracy of the vane anemometer reading. Three perforated plates are then removed from the model to check whether the flow inside the ESP behaves the same way as the flow behaves inside an unobstructed duct. The predicted velocity, shown in Fig. 10 is found as expected, that is, a high velocity in the middle and a low velocity noticed near the wall.

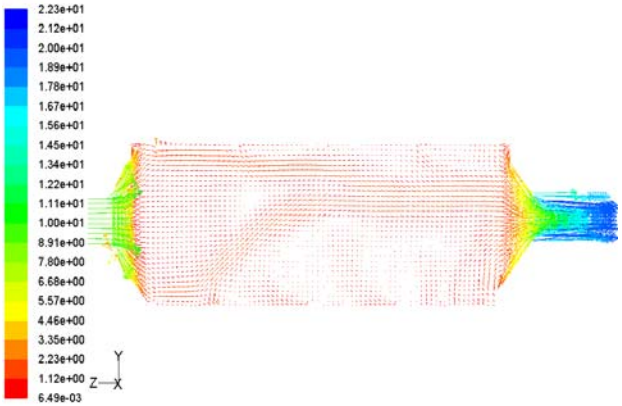

Fig.7 Velocity distribution at x=0m (symmetry plane) – side view section.

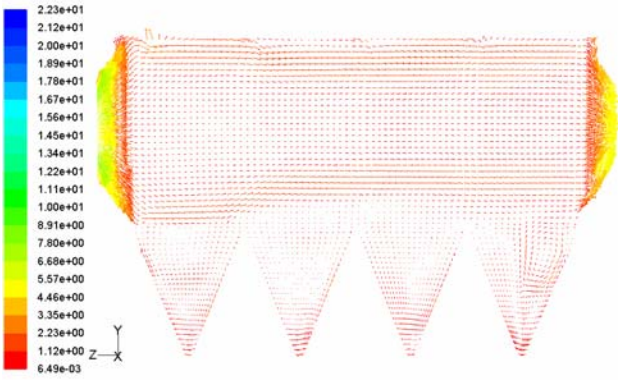

Fig.8 Velocity distribution at x=2.75m – side view section.

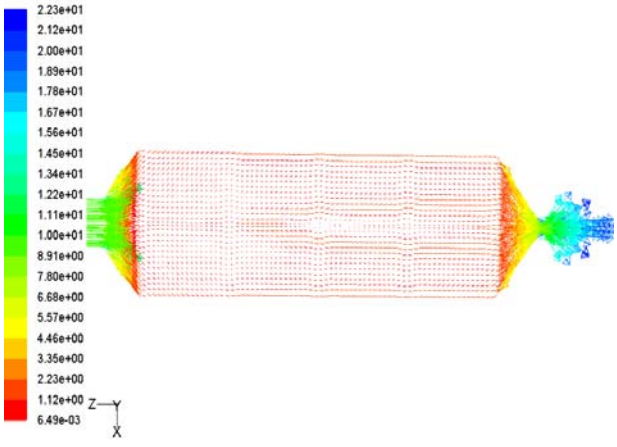

Fig.9 Velocity vectors at y=5.91m – plan view section.

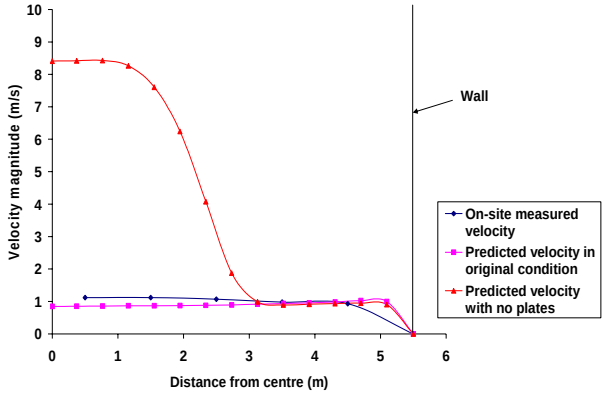

Fig.10 Velocity magnitude at y=5.91m (Plane 2). Comparison between the measured data and CFD prediction

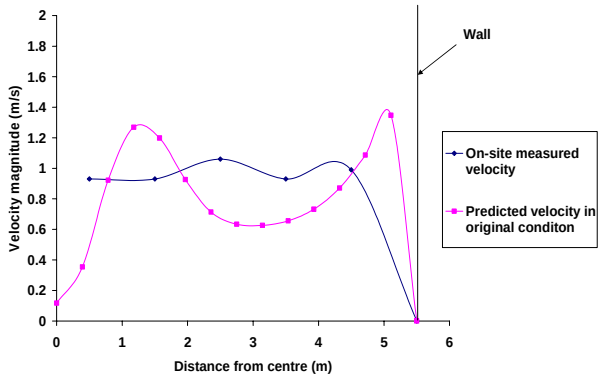

Fig.11 Velocity magnitude at y=5.91m (Plane 3). Comparison between the measured data and CFD prediction

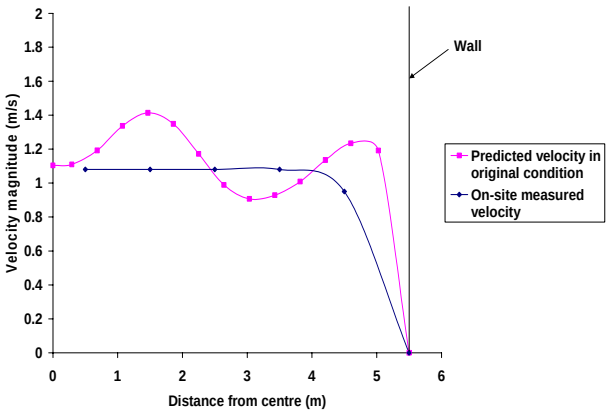

Fig.12 Velocity magnitude at y=5.91m (Plane 4). Comparison between the measured data and CFD prediction

According to the on going model the simulated velocity profile inside the collection chamber, which is not uniformly distributed rather streamlined through a small collection area with high flow velocity is a mismatch with the measured velocity distribution. The discrepancy may be associated with the course mesh size and lack of details of the exact geometry in the model. Hence more simulation is being carried out with finer mesh in order to achieve a better prediction. Further work on perforated plate is being carried out to predict the face permeability and pressure jump coefficient of the porous surface more accurately. It is expected that this will lead to a better match with the measured values and provide a good insight to the flow behavior inside the ESP.

5 Concluding Remarks

An on going CFD analysis for the full scale ESP is presented. Reynolds Stress Model for turbulence condition inside the ESP is applied. Numerically predicted velocities inside the ESP are compared with the measured data. As seen, these predictions are not the exact matches with the measured data. The deviations may be due to the course mesh, lack of details of exact geometry in the model, incorrect face permeability and pressure jump coefficient of the porous plates. Further simulation is being carried out introducing finer mesh and different face permeability and pressure jump coefficient of perforated plates in order to achieve a better prediction of flow behavior inside the ESP. Moreover, particle size distribution inside the ESP will be analyzed to explore the interaction of varying sized particles with flue gas. Study of such two-phase three dimensional flow under a charged confined space may give a good prediction on the effects of flow distribution on the particle residence time inside the ESP. This model can be useful in identifying options on operation and maintenance improvement activities by ESP tuning, optimizing flow distribution, field charging and rapping cycles and necessary plant modifications.

Acknowledgements

The authors would like to thank Stanwell Corporation Limited for supporting this work and providing on-site measured data.

References:

[1] M. J. Schwab, R. W. Johnson, Numerical design method for improving gas distribution within electrostatic precipitators, Proceedings of the American Power Conference, Vol. 56, 1994, pp. 882-888

[2] A.A.Varonos, J.S.Anagnostopoulos, G.C.Bergeles, Prediction of the cleaning efficiency of an electrostatic precipitator, Journal of Electrostatics, Vol. 55, 2002, pp. 111 – 133

[3] C.U.Bottner, M.Sommerfeld, Euler/Lagrange calculations of particle motion in turbulent flow coupled with an electric field, Proceedings of ECCOMAS Computational Fluid Dynamics Conference, 2001

[4] G. Gan, S. B. Riffat, Pressure loss characteristics of orifice and perforated plates, Experimental Thermal and Fluid Science, Vol. 14, 1997, pp 160-165

[5] K.S.P.Nikas, A.A.Varnos, G.C.Bergeles, Numerical simulation of the flow and the collection mechanisms inside a laboratory scale electrostatic precipitator, Journal of Electrostatics, Vol. 63, 2005, pp 423-443

[6] B.J.Dumont, R.G.Mudry, Computational fluid dynamic modeling of electrostatic precipitators, Proceedings of Electric power 2003 conference, 2003

[7] B.R.Munson, D.F.Young, T.H.Okiishi, Fundamentals of fluid mechanics, 4th ed., John Wiley & Sons Inc., NY, 2002

[8] Fluent 6.2 User's Guide, Fluent Inc., 2005

[9] R.Dattner, I.Donaldson, Gas distribution measurement report, Stanwell Power Station, 1992